Compositional dependence of ferromagnetism in (Al,Ga,Mn)As magnetic semiconductors

A. W. Rushforth, N. R. S. Farley, R. P. Campion, K. W. Edmonds, C. R. Staddon, C. T. Foxon, and B. L. Gallagher
School of Physics and Astronomy, University of Nottingham, University Park, Nottingham NG7 2RD, United Kingdom

K. M. Yu
Lawrence Berkeley National Laboratory, Berkeley, California 94720, USA

(Received 14 May 2008; revised manuscript received 16 July 2008; published 15 August 2008)

We report on a detailed study of the magnetic, electrical, and structural properties of the quaternary ferromagnetic semiconductor (Al,Ga,Mn)As. We investigate films with Al concentration y varying from 0.05 to 1, with a fixed total Mn density. The ferromagnetic transition temperature T_c decreases with increasing Al concentration, with no ferromagnetism observed at $y=0.5$ and $y=0.75$ for as-grown and annealed films, respectively. Detailed measurements identify three mechanisms giving rise to a suppression of T_c on alloying with Al: an increased tendency for Mn to occupy compensating interstitial sites, an increased stability of interstitials against annealing, and an increased localization of carriers. These studies serve as a test of the validity of theories of ferromagnetism in III-V semiconductors across different chemical compositions and represent a starting point for the development of new GaAs/(Al,Ga)As ferromagnetic heterostructures.

DOI: 10.1103/PhysRevB.78.085209 PACS number(s): 75.50.Pp

I. INTRODUCTION

The realization of ferromagnetism in III-V semiconductors by doping with Mn has led to the development of a new generation of electronic devices, based on tried-and-tested GaAs/(Al,Ga)As structures but also utilizing the spin degree of freedom.[1] In most such cases, Mn is incorporated in the GaAs layers, while the (Al,Ga)As layers serve as tunnel barriers. There is much less work on Mn doping of (Al,Ga)As. Early studies indicated that the incorporation of Al suppresses the ferromagnetic transition temperature T_c in arsenide ferromagnetic semiconductors, with T_c of only 40 K obtained in $Al_{0.17}Ga_{0.78}Mn_{0.05}As$ (Ref. 2) [compared to values exceeding 170 K in (Ga,Mn)As (Ref. 3)] and no ferromagnetic ordering observed for $Al_{0.96}Mn_{0.04}As$ (Ref. 4). However, the T_c in these systems is strongly dependent on the density of substitutional Mn moments as well as unwanted compensating defects, so that the effects of chemical composition on the ferromagnetism can be fully elucidated only through detailed materials characterization.

Ferromagnetism in III-V semiconductors is reliant on the acceptor nature of the substitutional Mn ions. The resulting holes mediate the ferromagnetic order between the localized Mn 3*d* spins, and the range of the Mn-Mn interaction is determined by the degree to which the carriers are extended or localized.[5] There is much interest in identifying and understanding trends across the III-V family. The highest T_c are observed for (Ga,Mn)As. Although the details of the electronic structure of this material remain somewhat controversial,[6,7] it may be expected that the relatively shallow Mn level introduces delocalized holes into the valence band.[3,5,7–9]The narrower-band-gapped materials (In,Mn)As and (Ga,Mn)Sb display magnetic and dc transport properties similar to those of (Ga,Mn)As but with a lower T_c due to weaker *p-d* hybridization.[9] In contrast, for the wider-band-gapped GaN, Mn is a deep acceptor. The resulting holes are strongly localized around the Mn ions, and the resulting T_c is very low [typically less than 10 K (Refs. 10 and 11)]. Mn-doped GaP appears to be an intermediate case, in which ferromagnetism with $T_c \sim 60$ K is observed together with insulating behavior and a gap in the photoconductivity spectrum, suggesting that the magnetic order in this system is mediated by holes with rather localized impurity-band-like character.[12]

Recently, a detailed theoretical investigation of hole-mediated ferromagnetism in both (Al,Ga,Mn)As and (Ga,Mn)(As,P) was reported by Masek *et al.*[13] The advantage of studying this combination is that AlAs and GaP have similar band offsets (and thus acceptor level positions) relative to GaAs but quite different lattice constants. Studies across this composition therefore allow a disentangling of the effects of these two parameters on the strength and range of the Mn-Mn interaction. From these calculations it was inferred that alloying with Al should affect T_c only weakly, while a sizable enhancement was predicted on alloying with P. In order to understand the validity of the assumptions underlying these (and other) predictions, it is essential to determine the range of applicability of the delocalized-hole picture as the band offset is increased from the GaAs case to the wider-gapped materials for well-controlled chemical compositions and minimal numbers of unintentional impurities and defects. This requirement has motivated the present work, in which we determine the properties of a set of (Al,Ga,Mn)As films with a wide range of Al concentrations.

The most important compensating defects in (Ga,Mn)As are Mn interstitial ions (Mn_I), which are double donors.[14] High concentrations of Mn_I can lead to substantial reductions in carrier density, magnetic moment per Mn ion, and T_c. It has been shown that Mn_I are rather mobile in (Ga,Mn)As and can diffuse out of the material on annealing in air at relatively low temperatures, comparable to the growth temperature ($\sim$200 °C).[15–18] This is a crucial step for obtaining (Ga,Mn)As films with the highest T_c ($\sim$150–180 K).[3,19] *Ab initio* calculations of the formation energy of Mn_I indicate that its concentration in a quaternary system such as (Al,Ga,Mn)As may be strongly affected by the composition.[13] In the following, we denote the composition of the layers under study as $(Al_yGa_{1-x-y}Mn_x)Mn_zAs$, where z represents the concentration of Mn_I per formula unit.

II. SAMPLE PREPARATION

The (Al,Ga,Mn)As films with various Al contents were grown on GaAs buffer layers on GaAs(001) substrates using low-temperature molecular-beam epitaxy. *In situ* reflection high-energy electron-diffraction (RHEED) measurements showed that the films remained two dimensional throughout the growth. During growth, the ratio of Mn to (Ga/Al) fluxes was set at a constant level corresponding to a nominal Mn concentration $(x+z)$ of 0.06. The Mn-doped layer thickness was 25 nm in each case. For layers with >30% Al, the films were capped with 20 nm of As, deposited at room temperature, to act as a barrier against oxidation. In addition, layers with 10% and 30% Al were grown both with and without an As cap to investigate whether the cap influences the properties of the magnetic layer. We found that the Curie temperature before and after annealing was not affected by the presence of the As cap. However the total moment was slightly higher in the capped films, consistent with the presence of a 1 nm oxidized layer at the surface of the uncapped wafer. After growth, the films were cleaved into pieces for measurements using x-ray diffraction (XRD), channeling Rutherford backscattering (c-RBS) and particle-induced x-ray emission (c-PIXE), superconducting quantum interference device (SQUID) magnetometry, and electrical transport. After each measurement, the pieces were annealed in air at 190 °C for 24 or 48 h, and the measurements were repeated on the annealed films.

III. RESULTS

The magnetic properties of the samples were determined using a Quantum Design SQUID magnetometer. The T_c was obtained from measurements of the remnant magnetization along the in-plane [110] and [$\bar{1}$10] and out-of-plane [001] axes versus increasing temperature after cooling down to 2 K in a 1000 Oe magnetic field. The results are shown in Fig. 1(a). For both as-grown and annealed samples, the T_c decreases with increasing Al concentration y. No remanence was observed for annealed films with $y=0.75$ or higher or for the as-grown film with $y=0.5$. We also find that as the Al concentration initially increases, the effect of increasing the anneal time from 24 to 48 h becomes substantially more pronounced. Figure 1(b) shows the difference ΔT_c between as-grown and annealed films. ΔT_c rises to a peak at $y=0.2$.

The easy axis of the as-grown films with $y=0.2$ or 0.3 is found to lie perpendicular to the plane. This is consistent with previous studies of (Al,Ga,Mn)As (Ref. 2) as well as insulating (Ga,Mn)As (Ref. 20). For as-grown films with smaller y as well as annealed films with $y\leq 0.5$, the easy axis is found to lie in the plane, as is typical for metallic (Ga,Mn)As films under compressive strain.[20]

Figure 2 shows resistivity versus temperature measurements obtained from Hall bars patterned from the uncapped (Al,Ga,Mn)As films. The observed transport properties are characteristic of (Ga,Mn)As materials on either side of the metal-insulator transition (MIT).[21] The resistivity and tendency toward insulating behavior increase with increasing Al concentration and decrease on annealing. For the metallic

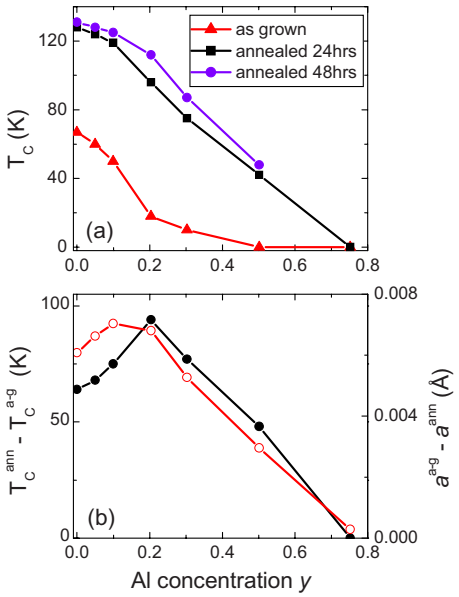

FIG. 1. (Color online) (a) Curie temperature obtained from remanence measurements versus Al concentration for as-grown films (triangles) and after annealing at 190 °C for 24 h (squares) and 48 h (circles). (b) Maximum changes on annealing in T_c (filled symbols, left axis) and relaxed lattice constant (open symbols, right axis).

films (annealed films with $y\leq 0.2$ and as-grown films with $y\leq 0.05$), the resistivity shows a sharp drop as the temperature is decreased below T_c, and the resistivity is finite at low temperatures. The as-grown films with $y\geq 0.2$ show insulating behavior with the resistivity strongly diverging at low temperatures. The as-grown film with $y=0.1$ and the annealed film with $y=0.3$ are close to the MIT.

High-resolution XRD measurements were obtained using a Philips X'Pert Materials Research diffractometer. $\omega-2\theta$ measurements of the as-grown and 48 h annealed (Al,Ga,Mn)As samples, extracted from reciprocal space maps at the GaAs(004) peak, are shown in Fig. 3. The broad peak marked with the dashed line corresponds to the thin (Al,Ga,Mn)As film and shows a clear shift with increasing Al content and on annealing. These measurements confirm that the Mn-doped layers are under compressive strain. Also, the data are well-described by fits obtained using the Philips SMOOTHFIT software package, with the composition and film thickness as fitting parameters, indicating the high structural quality of the layers. For most of the films the thickness extracted from the fits is in good agreement with the value of 25 nm estimated from the growth (to within ±2 nm). The exception is the (Al,Mn)As film, which appears to be significantly thinner (~17 nm) as grown and is barely measurable after annealing. This indicates that the (Al,Mn)As film is highly sensitive to oxidation, even with an As capping layer.

The relaxed lattice constants extracted from the fits are shown in Fig. 4. In both as-grown and annealed sets, the lattice constant has a strong and nonlinear dependence on the Al concentration. The lattice constant is reduced in the annealed films, consistent with an out-diffusion of interstitial Mn.[15,22]

The expansion of the lattice constant shown in Fig. 4 may be partially ascribed to the substitutional incorporation of Al,

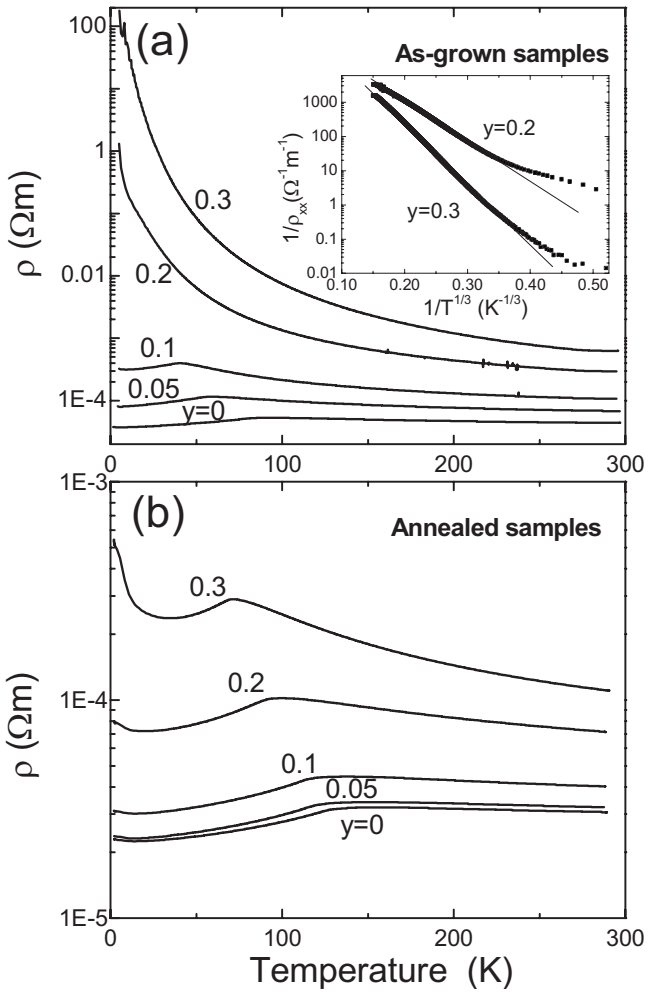

FIG. 2. Resistivity versus temperature for (Al,Ga,Mn)As films (a) as grown and (b) annealed. The Al concentration y corresponding to each curve is displayed in the figure. The inset of (a) shows $1/\rho$ on a logarithmic scale versus $T^{-1/3}$ for $y=0.2$ and 0.3.

due to the larger lattice constant of AlAs compared to GaAs. This effect can be accounted for using Vegard's law, $a = ya_{\mathrm{AlAs}} + (1-y)a_{\mathrm{GaAs}} + \alpha$, where $a_{\mathrm{AlAs}} = 5.661\,82$ Å and $a_{\mathrm{GaAs}} = 5.653\,68$ Å are the lattice constants of AlAs and GaAs, respectively, and the offset α is determined by the concentrations of substitutional and interstitial Mn as well as other defects.[23,24] The expected influence of substitutional Al is shown by the dashed lines in Fig. 4, where α is fixed at the value required to reproduce the experimental lattice constants of the as-grown and annealed (Ga,Mn)As films. Deviations from these lines indicate a change in the concentration and/or influence on the lattice of Mn_I or other defects. [Note that deviations from Vegard's law for AlAs-GaAs alloys[25] are much smaller than the observed deviations for the (Al,Ga,Mn)As films.]

In the as-grown films, the lattice constant increases sharply initially before following the Vegard's law slope for $y=0.2-0.5$ and decreases at higher Al concentrations. In the annealed films the lattice constant follows the Vegard's law expectation up to $y=0.1$, before increasing sharply up to $y=0.5$. The change in lattice constant on annealing, shown in Fig. 1(b), behaves similarly to ΔT_c, with the maximum

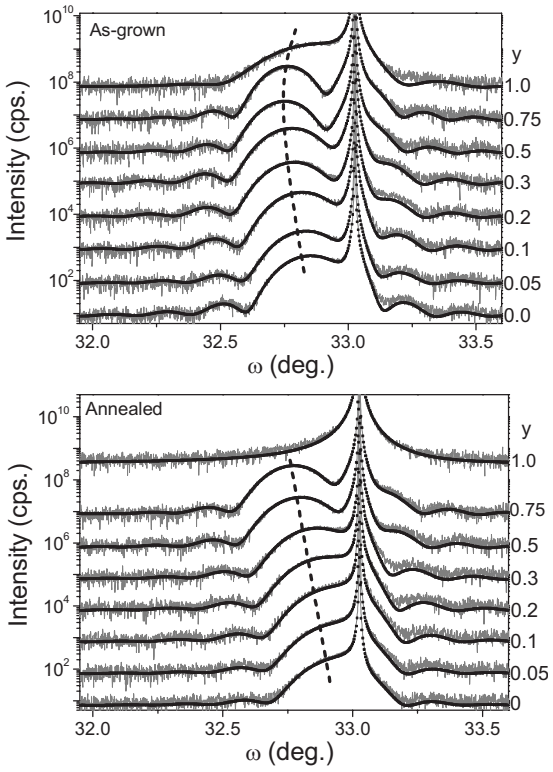

FIG. 3. X-ray-diffraction $\omega-2\theta$ scans for the 25-nm-thick (Al,Ga,Mn)As films. The lines are experimental data, the points are fits, and the dashed lines indicate the 004 peak corresponding to the film. The curves are offset in order of increasing Al concentration y, indicated by the numbers shown to the right of the figure.

change at around $y=0.1-0.2$ and a negligible change at $y=0.75$.

The locations of the Mn sites in As-capped films with $y=0.1$, 0.3, 0.5, and 0.75, as well as an uncapped (Ga,Mn)As film, were studied using ion channeling methods.[17] The substitutional, interstitial, and random Mn fractions, extracted from the normalized c-PIXE and c-RBS yields as a function of the tilt angle around the channeling axis, are shown in Fig. 5. The channeling measurements indicate that in the as-

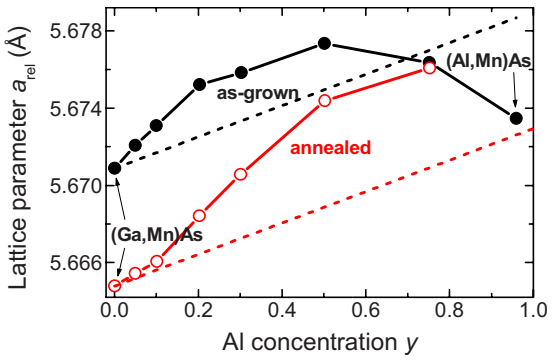

FIG. 4. (Color online) Relaxed lattice constants versus Al concentration. The filled symbols are for as-grown films and the open symbols are for annealed films. The dashed lines indicate the expected expansion of the lattice on Al incorporation according to Vegard's law, assuming a fixed offset due to the incorporation of Mn.

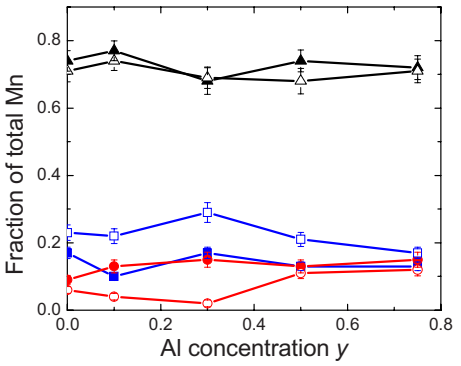

FIG. 5. (Color online) Fractions of Mn at substitutional (triangles), interstitial (circles), and random (squares) locations, as obtained from ion channeling measurements, as a function of the Al concentration y. The filled symbols are for the as-grown films and the open symbols are for after annealing.

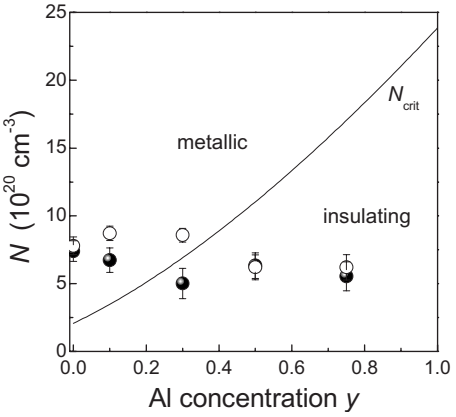

FIG. 6. Density of uncompensated acceptors, estimated from ion channeling measurements for as-grown (filled symbols) and annealed (open symbols) thin films, versus Al concentration. The solid line indicates the critical acceptor concentration separating metallic and insulating films, predicted by a simple model which accounts for the valence-band offset in GaAs-AlAs alloys.

grown films, around 10%–15% of the Mn is located on interstitial sites. Consistent with expectations, the effect of annealing is to increase the concentration of randomly located Mn ions at the expense of the interstitial fraction, while the substitutional fraction is not significantly changed. Although c-PIXE measurements do not give depth sensitivity, it is likely that the random Mn sites are located at the surface, due to reaction between out-diffused interstitial ions and the As cap.[18,26]

The results in Fig. 5 show that the interstitials are largely removed by annealing for low Al concentrations but are barely affected at high Al concentrations. This is consistent with the XRD results, which show that the change in lattice constant on annealing decreases with increasing Al concentration, indicating increasing stability of the interstitial Mn.

IV. DISCUSSION

From the results presented in Sec. III, we identify three factors which may give rise to the observed decrease in T_c with increasing Al concentration:

(1) *Increase in interstitial Mn concentration.* Mn_I are highly detrimental to ferromagnetism in (Ga,Mn)As due to compensation of both valence-band holes and available local moments.[3,14,18] The rapid initial increase in the lattice constant on alloying with Al indicates an increased tendency for interstitials to occur. References 23 and 22 give theoretical and experimental estimates of the expansion of the lattice constant due to Mn interstitials as $1.05z$ Å and $(0.6 \pm 0.2)z$ Å, respectively. The observed expansion of the lattice on going from $y=0$ to $y=0.1$ in the as-grown films (Fig. 4) would therefore correspond to an increase in the Mn_I concentration per formula unit of $\Delta z \sim 0.002$. This is consistent with the results of the ion channeling measurements within the experimental uncertainty. The increase in the Mn_I concentration will result in increased compensation and thus reduced T_c in the as-grown (Al,Ga,Mn)As films. However, if the interstitials are efficiently removed by annealing, then recovery of T_c should be possible. This is consistent with the behavior observed at low Al concentration ($y \leq 0.1$), where the T_c is significantly suppressed in the as-grown films but is only weakly dependent on y after annealing.

(2) *Increase in the stability of interstitial Mn against outdiffusion.* This is clearly demonstrated by the c-PIXE results, which show that annealing has little effect on the interstitial fraction for Al concentrations of 0.5 or more (Fig. 5). This is also consistent with the XRD measurements (Fig. 4) and the dependence of T_c on anneal time [Fig. 1(a)]. As a consequence, the high compensation at high Al concentrations is not reduced by annealing. This will contribute to the low T_c observed for large y. The increased stability may be related to the increasing ionicity of (Al,Ga)As alloys with increasing Al concentration, leading to deeper energy minima at the interstitial sites.

(3) *Localization.* The localized levels of transition metal ions in semiconductor alloys are pinned to an internal reference level or neutrality level, which is determined by the valence-band offset.[27,28] With increasing Al concentration, the valence-band offset increases, so that the Mn impurity level moves deeper into the band gap and the holes become localized around the Mn ions. This is consistent with the transition from metallic to insulating behavior observed with increasing y (Fig. 2). A crude estimate of the critical concentration N_{crit} of uncompensated impurities at which the metal-insulator transition occurs can be obtained by comparing the effective Bohr radius, $a_B=(\hbar^2/2m^*E_{a0})^{1/2}$, of an isolated acceptor with binding energy E_{a0} (=0.11 eV for Mn in GaAs), to the average impurity spacing $\sim N_{\mathrm{crit}}^{-1/3}$ (Ref. 7). Figure 6 shows the value of N_{crit} estimated from this simple picture as a function of Al concentration, using $E_{a0}=(0.11+0.45y)$ eV (reflecting the known binding energy in GaAs and valence-band offset in $Al_yGa_{1-y}As$ alloys). The values are scaled to yield the critical concentration of $\sim 2 \times 10^{20}$ cm^{-3} obtained for (Ga,Mn)As films.[8,29] The points in Fig. 6 are the densities of uncompensated acceptors in the studied films, estimated using $N=x-2z$, where x and z are the substitutional and interstitial Mn concentrations obtained from the c-PIXE measurements. This simple model repro-

duces the observed metallic behavior for $y \leq 0.1$ and the crossover from insulating to metallic behavior on annealing at $y=0.3$. None of the samples shows an activated form for the resistivity as a function of temperature. The as-grown samples with 20% and 30% Al show characteristics of hopping conduction. [See the inset of Fig. 2(a), illustrating the linear form of $1/\rho$ vs $1/T^{1/3}$. The gradient changes at around T_c.] This is consistent with the interpretation of carriers becoming localized for these Al concentrations. The strong localization of holes in the insulating regime means that carrier-mediated exchange interactions are very short ranged. As a result, the T_c is very low at high Al concentrations.

V. SUMMARY AND OUTLOOK

Our results indicate that T_c decreases on alloying (Ga,Mn)As with Al and that the decrease is at least partially attributable to a compositional dependence of the density and stability of compensating donors. Incorporating a small ($<\sim 20\%$) concentration of Al appears to result in an increase of the fraction of the incorporated Mn occupying interstitial sites, where they are detrimental to the ferromagnetic order.[14] For higher Al concentrations, the interstitial fraction does not show a further increase. However, the interstitial Mn becomes stable against annealing at 190 °C, where out-diffusion occurs in (Ga,Mn)As (Ref. 18). Therefore, the interstitials cannot be efficiently removed from the lattice, and compensation remains high in the annealed samples with high Al concentration.

The results for annealed films with low Al concentration ($<\sim 10\%$) are in qualitative agreement with the calculations presented in Ref. 13, with T_c decreasing only slightly with increasing Al. In these films, Mn_I are effectively removed by the low-temperature annealing process, and the remaining compensation is small. In the other investigated films, T_c decreases substantially as the Al concentration is increased. This may indicate that localization becomes increasingly important as the Al concentration is increased above 0.1–0.2, which would limit the validity of the model used in Ref. 13. However, it should be noted that there is significant compensation in the as-grown samples as well as annealed samples with $y>0.3$. If the hole concentration in these materials could be increased, by either increasing the substitutional Mn density or removing the unwanted compensating defects, then it may be possible to move toward the regime of metallic conduction in which the delocalized-hole picture may be appropriate.

ACKNOWLEDGMENTS

We acknowledge discussions with Tomas Jungwirth, Josef Kudrnovsky, and Jan Masek and funding from EU Grant No. IST-015728 and EPSRC-GB Grants No. GR/S81407/01 and No. EP/D051487. The work performed at LBNL was supported by the Director, Office of Science, Office of Basic Energy Sciences, Division of Materials Sciences and Engineering, of the U.S. Department of Energy under Contract No. DE-AC02-05CH11231.

[1] H. Ohno, F. Matsukura, and Y. Ohno, Solid State Commun. **119**, 281 (2001); M. Tanaka, H. Shimizu, T. Hatashi, H. Shimada, and K. Ando, J. Vac. Sci. Technol. A **18**, 1247 (2000).
[2] K. Takamura, F. Matsukura, D. Chiba, and H. Ohno, Appl. Phys. Lett. **81**, 2590 (2002).
[3] T. Jungwirth, K. Y. Wang, J. Masek, K. W. Edmonds, J. Konig, J. Sinova, M. Polini, N. A. Goncharuk, A. H. MacDonald, M. Sawicki, A. W. Rushforth, R. P. Campion, L. X. Zhao, C. T. Foxon, and B. L. Gallagher, Phys. Rev. B **72**, 165204 (2005).
[4] Z. Liu, J. De Boeck, V. V. Moshchalkov, and G. Borghs, J. Magn. Magn. Mater. **242**, 967 (2002).
[5] K. Sato, W. Schweika, P. H. Dederichs, and H. Katayama-Yoshida, Phys. Rev. B **70**, 201202(R) (2004).
[6] K. S. Burch, D. B. Shrekenhamer, E. J. Singley, J. Stephens, B. L. Sheu, R. K. Kawakami, P. Schiffer, N. Samarth, D. D. Awschalom, and D. N. Basov, Phys. Rev. Lett. **97**, 087208 (2006).
[7] T. Jungwirth, J. Sinova, A. H. MacDonald, B. L. Gallagher, V. Novak, K. W. Edmonds, A. W. Rushforth, R. P. Campion, C. T. Foxon, L. Eaves, E. Olejnik, J. Masek, S. R. Eric Yang, J. Wunderlich, C. Gould, L. W. Molenkamp, T. Dietl, and H. Ohno, Phys. Rev. B **76**, 125206 (2007).
[8] F. Matsukura, H. Ohno, A. Shen, and Y. Sugawara, Phys. Rev. B **57**, R2037 (1998).
[9] T. Dietl, H. Ohno, F. Matsukura, J. Cibert, and D. Ferrand, Science **287**, 1019 (2000).
[10] E. Sarigiannidou, F. Wilhelm, E. Monroy, R. M. Galera, E. Bellet-Amalric, A. Rogalev, J. Goulon, J. Cibert, and H. Mariette, Phys. Rev. B **74**, 041306(R) (2006).
[11] A. A. Freeman, K. W. Edmonds, N. R. S. Farley, S. V. Novikov, R. P. Campion, C. T. Foxon, B. L. Gallagher, E. Sarigiannidou, and G. van der Laan, Phys. Rev. B **76**, 081201(R) (2007).
[12] M. A. Scarpulla, B. L. Cardozo, R. Farshchi, W. M. Hlaing Oo, M. D. McCluskey, K. M. Yu, and O. D. Dubon, Phys. Rev. Lett. **95**, 207204 (2005).
[13] J. Masek, J. Kudrnovsky, F. Maca, J. Sinova, A. H. MacDonald, R. P. Campion, B. L. Gallagher, and T. Jungwirth, Phys. Rev. B **75**, 045202 (2007).
[14] J. Blinowski and P. Kacman, Phys. Rev. B **67**, 121204(R) (2003).
[15] T. Hayashi, Y. Hashimoto, S. Katsumoto, and Y. Iye, Appl. Phys. Lett. **78**, 1691 (2001).
[16] K. W. Edmonds, K. Y. Wang, R. P. Campion, A. C. Neumann, N. R. S. Farley, B. L. Gallagher, and C. T. Foxon, Appl. Phys. Lett. **81**, 4991 (2002).
[17] K. M. Yu, W. Walukiewicz, T. Wojtowicz, I. Kuryliszyn, X. Liu, Y. Sasaki, and J. K. Furdyna, Phys. Rev. B **65**, 201303(R) (2002).
[18] K. W. Edmonds, P. Boguslawski, K. Y. Wang, R. P. Campion, S. N. Novikov, N. R. S. Farley, B. L. Gallagher, C. T. Foxon, M. Sawicki, T. Dietl, M. Buongiorno Nardelli, and J. Bernholc, Phys. Rev. Lett. **92**, 037201 (2004).
[19] K. Olejnik, M. H. S. Owen, V. Novak, J. Masek, A. C. Irvine, J.

Wunderlich, and T. Jungwirth, Phys. Rev. B **78**, 054403 (2008).
[20] M. Sawicki, J. Magn. Magn. Mater. **300**, 1 (2006).
[21] A. Van Esch, L. Van Bockstal, J. De Boeck, G. Verbanck, A. S. van Steenbergen, P. J. Wellmann, B. Grietens, R. Bogaerts, F. Herlach, and G. Borghs, Phys. Rev. B **56**, 13103 (1997).
[22] L. X. Zhao, C. R. Staddon, K. Y. Wang, K. W. Edmonds, R. P. Campion, B. L. Gallagher, and C. T. Foxon, Appl. Phys. Lett. **86**, 071902 (2005).
[23] J. Masek, J. Kudrnovsky, and F. Maca, Phys. Rev. B **67**, 153203 (2003).
[24] K. Nakamura, K. Hatano, T. Akiyama, T. Ito, and A. J. Freeman, Phys. Rev. B **75**, 205205 (2007).
[25] D. Zhou and B. F. Usher, J. Phys. D **34**, 1461 (2001).
[26] M. Adell, J. Adell, L. Ilver, J. Kanski, J. Sadowski, and J. Z. Domagala, Phys. Rev. B **75**, 054415 (2007).
[27] J. M. Langer and H. Heinrich, Phys. Rev. Lett. **55**, 1414 (1985).
[28] T. Dietl, Semicond. Sci. Technol. **17**, 377 (2002).
[29] K. W. Edmonds, K. Y. Wang, R. P. Campion, A. C. Neumann, C. T. Foxon, B. L. Gallagher, and P. C. Main, Appl. Phys. Lett. **81**, 3010 (2002).